NPSAT1 Magnetic Attitude Control System

Barry S. Leonard
Naval Postgraduate School
699 Dyer Rd., Rm. 137
Code (AA/Lb)
Monterey, CA 93943-5106
bleonard@nps.navy.mil
ph: (831)656-7650; fax: (831)656-2313

Abstract

This paper describes the design and performance verification of a magnetically controlled smallsat being built by students and staff at the Naval Postgraduate School. The spacecraft (NPSAT1) will carry a number of experiments, including two sponsored by the Naval Research Lab and a commercial, off-the-shelf digital camera. Since NPSAT1 will be a secondary payload, it must be designed for a large mission box at minimum cost. Attitude control pointing requirements are less than 10° and an active magnetic control system is planned. NPSAT1 is manifested on the Department of Defense Space Test Program (STP) MLV-05, Delta IV mission, due to launch in January 2006.

Many spacecraft have employed magnetic sensing and actuation for attitude control. However, in most instances, the systems are designed with long gravity gradient booms for pitch and roll stabilization. The systems usually employ an extended Kalman filter when active damping is required. The NPSAT1 design employs a magnetic control system based on favorable moments of inertia realized by optimum equipment placement and ballast. The control system uses a standard quaternion control law for attitude control with a linear reduced order estimator for rate information. Attitude capture from initial orbit injection rates and steady state attitude errors less than 2° are demonstrated by simulation. The simulation is based on an 8th order magnetic field model and includes onboard computer sampling, torque rod command quantization, lag and saturation. Sensing and torque events are separated in time to prevent contamination of magnetometer data. Air bearing tests are planned for final performance verification. The control system hardware and software represent a minimum cost approach to spacecraft attitude control.

Nomenclature

b	= normalized magnetic field in orbit frame
B	= normalized magnetic field in body frame
Bdot	= derivative of **B** with respect to time
$\mathbf{B_t}$	= K_m **B** ~Tesla
B_x, B_y, B_z	= body frame components of **B**
B^2	= magnitude squared of **B**
g_x, g_y, g_z	= actuator time average gains
I_x, I_y, I_z	= principal moments of inertia
k	= **Bdot** gain
K	= controller gain, $[K_a \ K_b]$ (3x6)
K_m	= field "dipole strength"~Tesla
L_r	= reduced order estimator gain (3x3)
$\mathbf{m_p}$	= magnetic moment produced
$\mathbf{m_r}$	= magnetic moment requested
$q_1 \ q_2 \ q_3 \ q_4$	= quaternion elements
$\mathbf{T_p}$	= torque produced by the torque rods
x	= state vector (= ~ $\varphi, \theta, \psi, \dot{\varphi}, \dot{\theta}, \dot{\psi}$)
y	= measurement vector (= ~ φ, θ, ψ)
$\mathbf{T_r}$	= torque requested by the control law
u	= control vector
α	= true anomaly
β	= angle between sun and the orbit plane
Γ	= density variation factor
ν	= orbit angle WRT the sub-solar point
ρ, ρ_o, ρ_{max}	= atmospheric density, average and max
φ, θ, ψ	= yaw, pitch, roll Euler angle sequence
ω	= angular velocity WRT orbit frame
ω_e	= spin rate of Earth
ω_n	= line of nodes regression rate
ω_o	= orbit angular velocity

Introduction

Many control system actuator options are available to the spacecraft designer.[1,2] This paper considers only magnetic actuators because of their compatibility with smallsats. The sensing options considered include magnetometers, sun sensors, horizon sensors and MEMS gyros. Six options using various combinations of these sensors have been evaluated in a simulation using an IGRF[1,3,4] magnetic field of 8^{th} degree. All of the options meet NPSAT1 pointing requirement of less than 10º. The performance of each option would be enhanced by the addition of an ideal gravity gradient boom. The ideal boom would act as a rigid body in the presence satellite librations and thermal distortion. The selected option requires only magnetometers and magnetic torquers and does not require a boom at the 560 km mission altitude. The rigid body moments of inertia are modified by ballast to avoid resonance with the aero and solar disturbance torques at orbital frequency. This magnetic control approach does require an on board orbit propagator and tracking data on a weekly basis to meet pointing requirements. The selected control law is based on deriving rate from magnetometer data using a reduced order estimator[5] and time average[6] linearization of the torque rod control law.[2] This time average linearization enhances the application of linear analysis techniques. Consequently, an LQR approach is used to derive controller gains. Estimator gain selection is guided by simulation results. This approach is compared with a pole placement approach in the Appendix for the baseline spacecraft, a spacecraft with I_x slightly greater than I_y and for a spacecraft with a short boom. The transient response and steady errors of all three spacecraft are acceptable for this application. The controller and estimator gain calculations for all three spacecraft are based on a combined LQR pole placement approach.

The paper is presented in four sections. Section 1 describes the control system operation and design. Section 2 describes the system simulation. Section 3 presents simulation results and includes a performance comparison with options employing addition sensors. Section 4 discusses an error analysis of the baseline all magnetic system. The Appendix includes simulation details and the gain selection process.

I. Control System Description

The baseline control system functional block diagram is shown in Fig. 1. Ephemeris data is used to calculate components of the magnetic field vector **b** in orbital coordinates based on the International Geomagnetic Reference Field (IGRF of 8^{th} degree.)

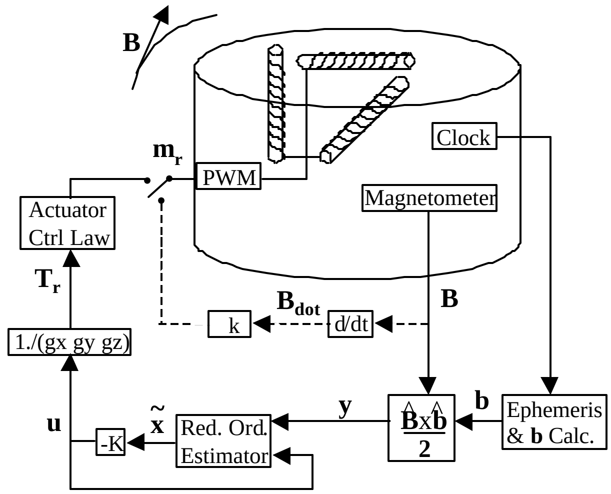

Fig. 1 Control system functional block diagram

An ideal quaternion control law[2]

$$\mathbf{u} = 2\,K_a\,\mathbf{y} + K_b\,w \qquad (1)$$

(where $\mathbf{y} = 2[q_1q_4 \quad q_2q_4 \quad q_3q_4]^T$) requires three axis attitude information from several sensors or extensive filtering of magnetometer data. Accurate calculation of w from magnetometer data is nontrivial.[7,8] An approximation for **y,** obtained directly from magnetometers and ephemeris data is given by:[7,8]

$$\tilde{\mathbf{y}} = \hat{\mathbf{B}} \times \hat{\mathbf{b}} / 2 \cong 2[q_1q_4 \;\; q_2q_4 \;\; q_3q_4]^T \qquad (2)$$

Eq. (2) can be viewed as a cross product steering law. The reduced order estimator[5] (ROE) uses this measurement, **y**, to estimate the state vector, **x**.

Selection of the gain K and the estimator gain L_r is described in the Appendix. Simulation data comparing the ideal and approximate approaches is presented in a later section. The actuator control law is given by[2]

$$\mathbf{m_r} = \mathbf{T_r} \times \mathbf{B} \,/\, B^2 \qquad (3)$$

and the torque on the spacecraft is given by[2]

$$\mathbf{T_p} = \mathbf{m_p} \times \mathbf{B} \qquad (4)$$

In the linear range of the magnetic torquers (i.e., when $\mathbf{m_p} = \mathbf{m_r}$), it can be shown that $\mathbf{T_p} = \mathbf{B}\,\mathbf{T_r}$

where,

$$\mathbf{B} = \begin{bmatrix} (By^2 + Bz^2)/B^2 & -BxBy/ B^2 & -BxBz/ B^2 \\ -BxBy/ B^2 & (Bx^2 + Bz^2)/B^2 & -ByBz/ B^2 \\ -BxBz/ B^2 & -ByBz/ B^2 & (Bx^2 + By^2)/B^2 \end{bmatrix}$$

The off diagonal terms of $\mathbf{B}$ have an average value of zero.[6] The diagonal terms, defined as g_x, g_y, and g_z respectively have average values that are a function of orbit inclination.[6] This dependence is shown in Table 1. Multiplying the components of $\mathbf{T_r}$ by the reciprocals of g_x, g_y, and g_z, respectively, yields an average value of $\mathbf{T_p}$ equal to $\mathbf{T_r}$ (i.e.; an ideal actuator, on the average). These gains influence performance of the controller and estimator gain selection process.

Table 1 Actuator Average Gains Versus Inclination at 560 km (IGRF 2000)

Inc.	g_x	g_y	g_z	Inc.	g_x	g_y	g_z
0	0.967	0	0.804	60	0.739	0.857	0.39
10	0.995	0.068	0.781	70	0.709	0.923	0.353
20	0.922	0.256	0.711	80	0.691	0.965	0.335
30	0.876	0.46	0.614	90	0.686	0.981	0.333
40	0.826	0.632	0.522	100	0.691	0.965	0.335
50	0.78	0.762	0.446	110	0.709	0.923	0.353

The **b** vector calculation requires latitude and longitude data accurate to approximately 0.1º (about 12 km in track). A coarse GPS system would be ideal; however, budget constraints forced the evaluation of alternatives. The two options being considered are an on-board orbit propagator (such as the SGP[9] model) and filtering of magnetometer and sun sensor data.[10] The SGP approach is currently favored since the code is reasonably compact and ground based updates are directly compatible with NORAD tracking data. The SGP model, with weekly updates from tracking data, should provide the required accuracy at the mission altitude of 560 km.

II. Simulation Description

A block diagram of the system simulation is shown in Fig. 2. Simulation parameters are summarized in the Appendix. The left upper part of the diagram shows the dynamics/kinematics being driven by disturbance and control torques.

The upper right part of the diagram shows the generation of the circular orbit true anomaly, $\alpha=\alpha_o+\omega_o t$, and the location of the Greenwich meridian with respect to the right ascension of the ascending node, $\lambda=\lambda_o+(\omega_e-\omega_n)t$.

Initial simulation work was based on a simple dipole model of the Earth's magnetic field. However, this model yielded very optimistic result and was replaced by an 8th degree IGRF model.

Components of the magnetic field vector are computed in latitude and longitude increments of five and ten degrees respectively for the mission altitude. This data is incorporated in a double look-up table and transformed into orbit coordinates of the **b** vector. The Orbit to Body Transformation provides the body frame field vector, **B**. The gravity-gradient, solar and aero torques are calculated in the Environmental Torques block. The location of the sub-solar point with respect to the right ascension of the ascending node, $\nu=\nu_o+\omega_o t$, allows calculation of day-night density variation[6] (see Appendix).

The lower part of Fig. 2 shows the spacecraft hardware and software. The lower right part of the diagram repeats the magnetic field model, discussed above, for the purpose of evaluating the impact of ephemeris and magnetic field model errors. The lower left part of the diagram contains the Torque Rods, Magnetometers and the two control modes. The initial control mode,[11] $\mathbf{m_r}$=k **Bdot**, reduces launch vehicle tip-off rates rapidly. The second mode provides attitude capture. Switching between modes will be controlled from the ground.

III. Simulation Results and Comparison of Options

Fig.3 shows rate and attitude versus time. The upper traces are without the Bdot control mode. The center traces use Bdot for 10,000 sec. The lower traces use Bdot for 20,000 sec. While these results show convergence without Bdot, rate damping is clearly improved with Bdot. In addition, Bdot convergence to low rates can be proven by analysis.[11,12] The Bdot mode damps rates but can not accomplish three axis attitude pointing. The second mode, referred to as the reduced order estimator (ROE) reduces attitude errors to about 1.5º (error primarily due to aero/solar torques).

The simulation was expanded to examine control options using additional sensors. A summary of the options and their characteristics is presented in Table 2.

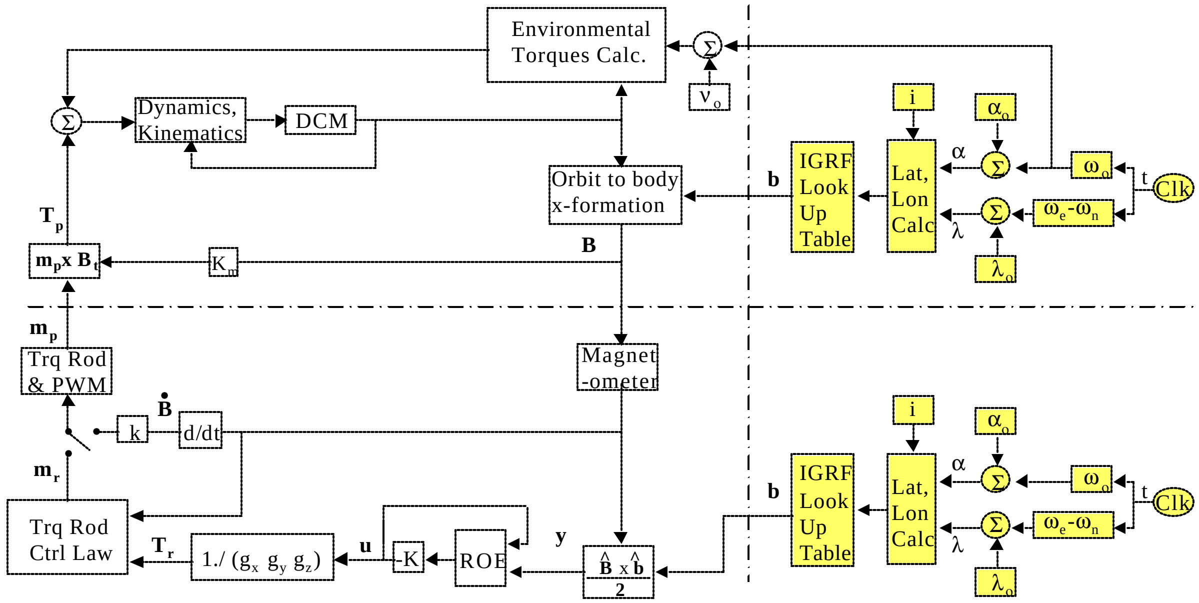

Fig. 2 Simulation Block Diagram

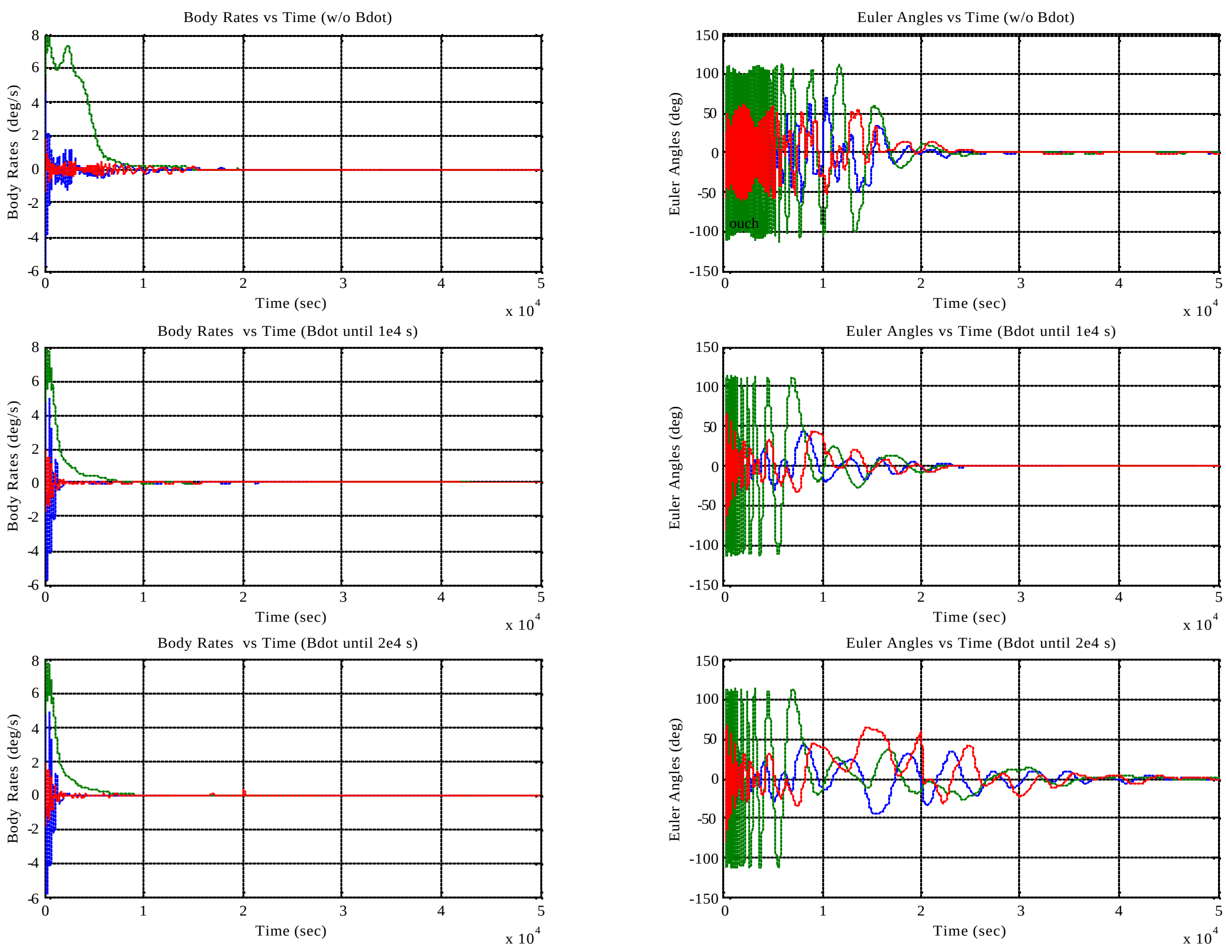

Fig. 3 Simulation Results

Table 2 Performance and characteristics of sensing options.

Option	Attitude Data Day	Attitude Data Night	Rate Data	SS Error ~deg	Acquisition Time~revs*	Option Characteristics Sensor Suite	Power ~W	Δcost ~K$	Δmass ~kg
1**	Mag	Mag	Estimator	1.5	5 to 24	Mag	1.2	----	----
2***	Quat	Mag	↓	1.3	↓	Mag + SS	1.8	6	0.9
3	Quat	Quat	↓	0.4	↓	Mag + HS	2.2	80	1
4	Mag	Mag	Gyros	0.6	4 to 8	Mag + Gyro	4.6	11	0.2
5	Quat	Mag	↓	0.5	↓	Mag+SS+Gyro	5.2	17	1.1
6	Quat	Quat	↓	0.4	↓	Mag+HS+Gyro	5.6	91	1.2

* Acquisition time is initial condition dependent (attitude, rate, true anomaly and lat./lon.)

** Magnetometer based control law; *** Quaternion based control law (Mag + SS or HS)

Δcost = hardware cost only (doesn't include I & T); Mag=magnetometer,SS=Sun senor, HS=horison sensor

Option 1 corresponds to the data in the lower part of Fig. 3 and uses only magnetometer data. Option 2 assumes perfect quaternion data during the day but only magnetometer data during eclipse. Option 3 assumes perfect quaternion data both day and night. All three of these options use Bdot, then the ROE. Options 4, 5, and 6 repeat Options 1, 2 and 3 but the ROE is replaced with ideal rate gyros to measure body rates. Clearly, the gyros provide better performance; however, they require more resources.

V. Error Sources and Impact

All of the options mentioned above are subject to errors that degrade their steady state accuracy. An error analysis of Option 1 is summarized in Table 3. The simulation was expanded to evaluate most of the error contributors. A modulation approach was used to avoid modeling torque rod corruption of magnetometer data. The torque rods are used at a 5% duty cycle, every two seconds. This provides adequate torque rod decay time (approximately 40 time constants). Results indicate an RSS error of 3.4º and a worst on worst error of 8.8º. While the error analysis requires further verification with actual hardware, initial results indicate pointing requirements are achievable.

V. Conclusions

A low cost control system for small satellites has been described. The system requires a three-axis magnetometer, three magnetic torque rods and simple on board calculations. The system does not require a boom or complex filter. Attitude information is derived from the cross product of the measured and predicted magnetic fields.[7,8] Rate information is derived by extending a SISO reduced order estimator[5] to this MIMO system. Weekly tracking data updates, to the SGP orbit propagator, provide a degree of autonomy. The system achieves the required pointing accuracy and compares favorably with options of greater complexity. A process has been outlined for calculation of magnetic system controller and estimator gains (see Appendix).

Table 3 Error Analysis Results

Error Source		Allocation	Units	Error ~deg
Magnetic Field Model*		Δ 1.5yrs	nT	0.8
Ephemeris Generator :		12	km	
Latitude Uncertainty		0.1	deg	0.1
Longitude Uncertainty		0.1	deg	0.1
Orbit Eccentricity		0.0005	deg	0.07
Magnetometer:	Accuracy **	0.5	%	0.37
	Alignment	0.25	deg	2
	Linearity **	0.15	%	0.1
	Noise**	20	pT	0.1
	Orthogonality	0.25	deg	1.7
	Bias**	250	nT	1
Torque Rod Orthogonality		1	deg	0.05
Mag Sample / Torque Rod Lag		0.01	sec	0.01
Ascent Shift		1	mm	0.2
Disturbance Torques (cm-cp)		8	mm	1.6
MOI Uncertainty		0.01	$kg.m^2$	0.6
* DGRF vs. IGRF			WOW	8.8
**Billingsley TFM100G2 Spec.			RSS	3.42

<u>**Appendix**</u>

Disturbance Torques

The atmospheric density variation from eclipse to sunlight can be expressed as:[6]

$$\rho = \rho_o \Gamma^{\cos\nu} \qquad \text{(A1)}$$

Eq. (A1) applies when the sun is in the orbit plane (i.e., β=0). For nonzero β, Eq.(A1) has been modified to provide a smooth transition from β = 0 to β = pi/2 as follows:

$$\rho = \rho_o \Gamma^{\cos\nu\cos\beta} \qquad \text{(A2)}$$

Expressing Eq. (A2) in terms of the orbit max density (assumed to occur at $\nu = \beta = 0$)

$$\rho = \rho_{max}\Gamma^{(\cos\nu\cos\beta-1)} \qquad \text{(A3)}$$

Eq. (A3) was used to calculate aero torques with Γ=1.5.[6] Conservative solar torque was also included in the simulation. Future work will assess the value of incorporating these disturbance torques into the estimator.[12]

Simulation Parameters

The simulation data is summarized in Table A1.

Table A1 Simulation Parameters

Parameter & units	Value
Altitude~km	560
Inclination ~deg	35.4
Density~kg/m^3	2.21E-13
Cd	2.5
Area~cm^2	[2674, 2674, 1927]
(cp-cm)~mm	[2, 2, 8]
Ixx~kg.m^2	5
Iyy~kg.m^2	5.1
Izz~kg.m^2	2
Ixy=Ixz=Iyz (nom.)	0
k	200
Km~ Tesla	2.30E-05
Trqr saturat'n.~ A.m^2	30

Gain Selection Process

This section describes three approaches for selecting the controller gain, K, and the estimator gain, L_r. The design was driven by a requirement to minimize response to disturbance torques at orbital frequency. The gain selection process actually began by arranging equipment within the spacecraft such that favorable moments of inertia were achieved (i.e., move the open loop roots as far away from ω_o as practical). This was accomplished while minimizing cross products of inertia and the distance between the centers of pressure and mass. The average torque gains[6] (g_x, g_y, g_z) provide time average linearization and enhance linear analysis techniques.

The controller gain, K, was initially selected using a standard LQR approach to minimize the time integral of:

$$x'Qx+u'Ru$$

The matrix Q was selected as the identity matrix. The three diagonal elements of R were selected as [1 4 0.004] to emphasize reduction of the yaw error. The REO gain, L_r, was selected as a diagonal matrix. The three elements of L_r were varied to achieve maximum damping in the presence of noise (a situation analogous to the "lead lag" ratio in a SISO system). The resulting estimator and controller roots are shown in Table A2.

Results of a second approach using pole placement are also summarized in Table A2. In this approach, the controller and estimator gains are calculated with a MIMO pole placement routine. Selection of these controller poles (round off of the LQR poles) would have been difficult without the LQR produced values. A third approach combines LQR and pole placement as follows:

Use an LQR routine to select K, with Q as the 6x6 identity matrix and R as a 3x3 diagonal matrix. Vary the three elements of R to achieve best performance for reasonable control effort. The LQR routine also outputs the three pairs of controller Eigenvalues. Use the norm of each pair of these Eigenvalues as a base set of estimator poles. Multiply this base set by a factor between 6 and 10 (high factors produce greater damping but greater noise response). Use the pole placement routine to calculate L_r.

Table A2 Eigenvalues and Gain Selection

System	Equation	Eigenvalues/wo			
		LQR *		Pole Placem't	
		Re part	Im part	Re part	Im part
Plant	A	0	+- 1.687	0	+- 1.687
		0	+-0.2087	0	+-0.2087
		0	+-1.328	0	+-1.328
Controller	A-BK	-8.775	+-8.801	-8.8	+-8.8
		-1.054	+-1.876	-1.1	+-1.9
		-0.648	+-1.478	-0.65	+-1.5
ROE**	A_{bb}-$L_r$$A_{ab}$	-82.96	0	-74.6	0
		-49.79	0	-13.2	0
		-41.48	0	-9.81	0

* Q=6x6 identity matrix, R=Diagonal matrix (1 4 0.004), L_r=Diagonal matrix (0.09 0.045 0.054)

**Reduced order estimator: A_{bb} , A_{ab} from partitioned A matrix as follows: A_{bb}= rows 4-6, columns 4-6; A_{ab}= rows 1-3, columns 4-6.

A= plant matrix (6x6) ; B= control input matrix (6x3)

The LQR weighting matrices shown in (Table A2) were used with two other sets of moments of inertia, namely: [Ix Iy Iz] = [5.7 5.6 2.2] and [20 20 2.2]. No adjustment to the simulation was required for the first set. Even though Ix>Iy, the results are satisfactory with steady state errors only slightly worse (0.1°) than the baseline set. The second set, equivalent to adding a short boom, required changing the R diagonal matrix to (2.1 4 0.0011) to produce comparable results. The combined approach still requires some iteration to find the best R. However, L_r is calculated by the pole placement routine.

Table A3 LQR / Pole Placement Code

```
Q=eye(6);    R=[1  0 0;0 4 0;0 0 .004]
[K,S,e]=lqr(A,B,Q,R)
pe=-6*[norm(e(1)) norm(e(3)) norm(e(5))]
Lr=place(Abb',Aab',e)'
```

Code used in the LQR / Pole Placement approach is summarized in Table A3.

Acknowledgments

The author acknowledges support from students and staff at the Naval Postgraduate School.

References

1. Wertz, J. R., "Spacecraft Attitude Determination and Control", Kluwer Academic Publishers, Boston, MA, 1994, pp. 779-781
2. Sidi, M. J., "Spacecraft Dynamics and Control", Cambridge University Press, 1997, p. 129, p. 156.
3. International Association of Geomagnetism and Aeronomy, Division V, Working Group
4. Revision Of The IGRF for 2000-2005,
5. Franklin, G. F., Powell, J. D., Emami-Naeini, A., "Feedback Control Of Dynamics Systems", Addison Wesley, 1988, pp. 352-356
6. Martel, F., Pal, P. K., and Psiaki, M., "Active Magnetic Control System for Gravity Gradient Stabilized Spacecraft", Second Annual AIAA/USU Conference on Small Satellites, (26-28 September 1988, Logan, UT), Washington, DC: AIAA.
7. Landiech, Philippe, "Extensive Use of Magnetometers and Magnetotorquers for Small Satellites Attitude Estimation and Control, 18th Annual AAS Guidance and Control Conference, Keystone, Colorado, Feb 1-5, 1995, AAS95-012.
8. Psiaki, M. L., Martel, F., and Pal, K. P., "Three–Axis Attitude Determination via Kalman Filtering of Magnetometer Data", Journal of Guidance, Control and Dynamics, Vol. 23, No. 3 pp 506-514.
9. Hoots, F. R. and Roehrich, R. L., "SPACETRACK REPORT NO.3, Models for Propagation of NORAD Element Sets", December 1980, Compiled by TS Kelso, 31 Dec 1988.
10. Jung, H. and Psiaki, M. L., "Tests of Magnetometer/Sun Sensor Orbit Determination Using Flight Data", Journal of Guidance, Control and Dynamics, Vol.25, No.3 pp. 582-590.
11. Stickler, C. A. and Alfriend, K. T., "An Elementary Magnetic Attitude Control System", Journal of Spacecraft and Rockets, 1976, pp 282-287.
12. Wisniewski, R., and Blanke, M., "Fully Magnetic Attitude Control for Spacecraft Subject to Gravity Gradient", Automatica 35 (1999) pp. 1201-1214.